Article

Synthesis of Quaternary-Ammonium-Lignin-Based Ionic Liquids and Comparison of Extraction Behavior of Co(II) and Ni(II) with 2-Ethylhexyl Phosphoric Acid Mono-2-Ethylhexyl Ester

Guijiang Li * and Wenze Xu

College of Chemical and Biological Engineering, Shandong University of Science and Technology, Qingdao 266590, China; 202383090047@sdust.edu.cn
* Correspondence: skd992045@sdust.edu.cn

Abstract: The escalating demand for cobalt in modern industry necessitates the recycling or extraction of this resource for sustainable development. Despite the abundance of lignin in nature, its utilization remains low, highlighting the need to enhance its value-added potential. This study focuses on the synthesis of quaternary ammonium lignin (QAL) and 2-ethylhexyl phosphoric acid mono-2-ethylhexyl ester (P507) as ionic liquid (QP–IL) compounds for the extraction of metal ions. A comparison of the extraction behavior of Co(II) and Ni(II) from chloride solution between QP–IL and P507 revealed varying extraction ratios under different conditions, with QP–IL demonstrating a higher cobalt extractability than P507. Furthermore, under identical conditions, QP–IL exhibited superior Co/Ni separation performance ($\beta_{Co/Ni}$) compared to P507. Ultimately, QP–IL proved to be more effective than P507 in separating cobalt from mixed solutions.

Keywords: quaternary ammonium lignin; ionic liquid; separation; cobalt; nickel

1. Introduction

Lignin, which is abundant in nature, has a very low utilization rate of approximately 2%. Most of the remaining lignin is either discarded or used as fuel. Due to its complex and heterogeneous structure, lignin exhibits low solubility in conventional organic solvents and water, which hinders its practical application. The modification of lignin is crucial for broadening its application scope. Lignin possesses several advantages, including the presence of beneficial functional groups such as aldehyde, methoxy, hydroxyl, carbonyl, phenolic, and carboxyl; low cost; high specific surface area and stability; biodegradability; and accessibility [1]. Consequently, lignin or modified lignin serves as a promising and environmentally friendly resource with numerous safe and effective applications, including as an antibacterial agent [2], adhesive [3], reinforcing agent [4], sustained-release agent [5], petroleum industry [6], supporting medium [7], etc. Lignin acts as a green support for the production of effective heterogeneous catalysts such as lignin-SO$_3$Sc(OTf)$_2$, lignin-SO$_3$Cu(OTf), and lignin-IL@NH$_2$. The synthesized LS-IL@NH$_2$ has been employed in the realm of catalysis and demonstrated a satisfactory catalytic performance [7,8]. Several studies suggest that modified lignin particles may be appropriate for targeted tumor and cancer treatments, as well as gene therapy [9]. Lignin originates from the process of photosynthesis and is eventually decomposed into carbon dioxide, which is a "zero-carbon" substance. Further research is needed to explore the development and utilization of lignin to meet carbon neutrality requirements. The high-value utilization potential of lignin requires additional investigation.

Although not as common as some other elements like iron or calcium, cobalt and nickel are still present in the Earth's crust and are often exploited in various industries. Typically, they often coexist in ores, copper converter slag [10–14], nickel slag, deep-sea manganese nodules [15,16], special alloy materials [17,18], battery materials [19–22], catalysts, sludge,

and waste water [23]. The escalating demand for cobalt and nickel due to economic expansion has led to resource depletion and subsequent price hikes; notably, cobalt is considered the most valuable element [24]. Moreover, a huge number of batteries containing cobalt or nickel have been generated worldwide and widely used in modern electronic devices. The spent battery can release toxic organic compounds which then result in serious environmental problems and public health if disposed of improperly [25,26]. Therefore, the recovery and utilization of cobalt is becoming more and more important, and it is vital to eliminate possible pollutants, as well as to produce it sustainably [19,21,27,28].

The separation and purification of cobalt from its aqueous form pose significant challenges due to the various origins, intricate parts, and comparable physical and chemical characteristics. A wide variety of separation strategies has been developed to recover valuable metals and eliminate pollution by chemical precipitation [29,30], solvent extraction [31–34], resin exchange [35], membrane separation [36], and bio-recovery [37]. The chemical precipitation method, which was previously the earliest option for cobalt and nickel separation, is now rarely used alone in modern processes due to the similar solubility and coprecipitation behavior of $Co(OH)_2$ and $Ni(OH)_2$.

The primary method of nickel and cobalt separation in the industrial sector, solvent extraction is an efficient and pliable technique that is based on the different distribution components to be separated from two immiscible liquid phases, typically water and an organic solvent [38]. In comparison with other processes, it is both efficient and flexible, making it the most effective choice.

The separation of cobalt and nickel was gradually enhanced by employing three extraction acids, Di(2-ethylhexyl)phosphoric acid (D2EHPA or P204) [39,40], hexyl phosphonic acid mono-2-ethyl-hexyl ester (*P507* or *PC88A*) [41], Bis(2,4,4-trimethylpentyl)phosphinic acid (Cyanex272) [42]. Among these acids, D2EHPA was the most commonly used solvent. D2EHPA can extract various metallic cations from various Carboxylates [43], Citrate [44–46], chloride [47], nitric [48,49], and sulfate [50,51] solutions. After the first commercial process using D2EHPA, P507 was developed and widely used in base-metal solvent extraction [41]. The single extraction tests revealed a Co/Ni separation factor of more than 350 and a Co stripping efficiency of 99.5% when optimal extraction was applied [52,53]. Moreover, the efficacy of P507(PC-88A) in the recovery of cobalt from various sulfate and chloride solutions with a wide variety of Ni/Co ratios was demonstrated through its chemical stability, reutilization, and low solubility in aqueous media. Additionally, Cyanex 272 has been proven capable of separating Co from Ni at low Co/Ni ratios [42,54], as well as selectively extracting cobalt from LIBs containing Co, Li, Ni, and metal ion impurities such as copper, iron, and aluminum [55,56].

Tertiary amine and quaternary ammonium salts are extensively utilized as amine extractants, employing anion exchange or ion association as metal ion extraction process [57,58]. Cobalt could be efficiently extracted (93.6%) from chloride leach liquors of spent nickelmetal hydride (Ni-MH) batteries in two stages using Alamine 336 [59]. Furthermore, 97.5 wt.% of Co(II) could be extracted using Alamine 336 from leaching spent Ni/Cd batteries with hydrochloric acid [60].

The oxime extraction agent was widely recognized for its extensive application in copper extraction [61]. However, it also exhibits high selectivity in nickel extraction. By employing LIX 84-I as the extractant, a single-step process achieved over 99% nickel extraction from ammonium-containing solutions with a phase ratio of 1.0 [62].

The solvent extraction is highly efficient due to its ability to selectively differentiate the metal contents in wastes or ores compared with other methods. Currently, it is one of the most popular methods used for the removal or separation of metallic species from the mixed-metal aqueous phase [24]. Moreover, it has also been successfully applied for the recovery of cobalt or nickel from various resources [63]. To achieve optimal efficiency, a complete flowsheet comprising one or more methods should be employed for the separation of cobalt, nickel, and other metal ions instead of relying solely on a single

approach. Furthermore, future development should focus on exploring novel materials and technologies.

Despite the feasibility of solvent extraction, persistent concerns remain regarding its safety and environmental implications. In particular, the volatility and combustibility of solvents give rise to substantial apprehensions. Extensive research efforts have been dedicated to exploring substitutes for organic solvents with the aim of bolstering the sustainability of this approach [64]. Ionic liquids, which are substances consisting solely of cations and anions with a melting point below 100 °C, have been recognized as innovative solvents. Diverse ionic liquids have demonstrated efficacy in accomplishing successful liquid-liquid extraction for Co/Ni separation [65–67], such as [A336][CA-12], [A336][P507], [P66614][PF6], etc. Nevertheless, factors such as acidic conditions (pH < 0), a high concentration of chloride ions (>6 mol·L^{-1}), a large volume, and high viscosity pose limitations on their applicability [66]. The search for novel ionic liquids is currently being pursued by numerous researchers.

Therefore, in this study, the conversion of lignin into a cationic form was achieved by the inclusion of quaternary ammonium groups that could interact with P507, thus generating new ionic liquid. Subsequently, QP–IL and P507 were used to evaluate the extraction and separation ability of Co(II) and Ni(II) from weak chloride media.

2. Materials and Methods

2.1. Materials and Reagents

Two components of the experiment's procedure were separated: synthesis and extraction. Lignin was supplied by Shanghai C-reagent Biotechnology Co., Ltd. (Shanghai, China) From sinopharm chemical reagent Co., Ltd., (Shanghai, China) chemicals for the synthesis of ionic liquid, such as N,N-dimethyltetradecylamine (DT), epichlorohydrin (EH), sodium ethanol, and 2-ethylhexyl phosphonic acid mono-2-ethylhexyl ester (P507), were procured. All the inorganic compounds were analytical regents. Cobalt chloride and nickel chloride were produced by kelong chemical Co., Ltd.(Chengdu, China), while TCI chemical Co., Ltd.(Shanghai, China) supplied NaOH and HCl to adjust the aqueous acidity. The standard multi-component solutions (100 µg/mL) of Co(II), Ni(II), Cu(II), Fe(II), and Mg(II) were from merch Co., Ltd.(Shanghai, China), The organic diluent kerosene was obtained from Aladdin Biochemical Technology Co., Ltd. (Shanghai, China) All chemicals were used without any purification.

2.2. Synthesis of QP–IL

Two stages were needed to synthesize the QP–IL, and the scheme is shown as Scheme 1.
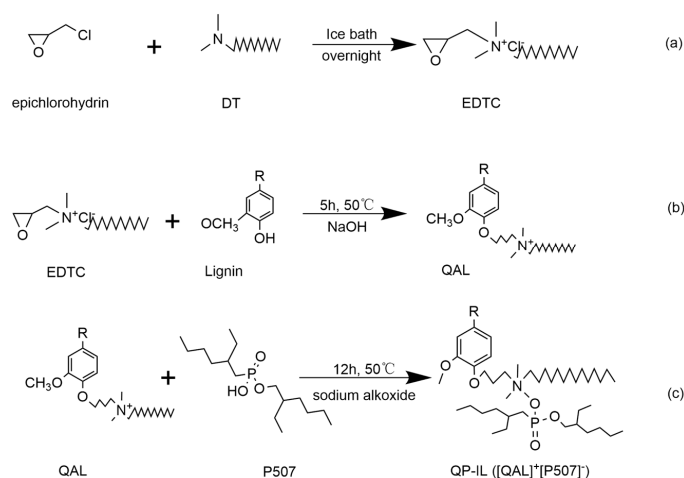
Scheme 1. Synthesis schemes of QP–IL. (**a**) synthesis of epichlorohydrin dimethyltetradecylamine chloride(EDTC). (**b**) synthesis of quaternary ammonium lignin (QAL). (**c**) synthesis of quaternary–ammonium–lignin–based IL(QP–IL).

2.2.1. Synthesis of Quaternary Ammonium Lignin (QAL)

Equipped with a condenser and stirrer, a three-neck flask was utilized to transfer the mixture of N,N-dimethyl tetradecyl amine (DT) and epichlorohydrin (EH)with a molar ratio of 5:3.5 in an ice–salt bath (NaCl/ice = 1:3) for 1.5 h. Subsequently, the reactants were left to react completely for an overnight period. Silver nitrate can detect epoxypropyl Dimethyl tetradecyl amine Chloride (EDTC) in a white precipitate, thus making it ready for the production of quaternary ammonium lignin.

A warm bath at 80 °C was used to react 50 mL of a sodium hydroxide solution with 0.4 g of lignin for 20 min. Subsequently, EDTC was blended into the reaction system, and the reaction was conducted with steady magnetic stirring for 5 h at 50 ± 5 °C until a brown emulsion was obtained. The mixture was centrifuged to obtain the QAL. The chemical reaction is demonstrated in Scheme 1a,b.

2.2.2. Synthesis of Quaternary–Ammonium–Lignin–Based IL (QP–IL)

[QAL][OH]: A total of 10 g QAL was dissolved in 100 mL of ethanol, and added dropwise into the ethanol solution containing sodium alkoxide. The solutions were stirred for 4 h at 50 °C. Afterwards, the mixture was centrifuged at 8000 r/min for 10 min to eradicate the white precipitate. Finally, the filtrates were shaken with equal volume of deionized water for an hour to obtain [QAL][OH] by the hydrolysis of [QAL][OR] [68].

QP–IL: After vigorously stirring a mixture of [QAL][OH] (0.12 mol/L) and P507(mole ratio is 1.1:1) for 12 h at 50 °C under reflux, it was left to settle. Subsequently, a layer of aqueous material was formed at the bottom. The upper phase was then poured into a vacuum rotatory evaporator (353 K, 20 mbar, 60 min) to eliminate any residual water and ethanol. The chemical reaction is demonstrated in Scheme 1c.

2.3. General Procedure for Co and Ni Extraction

Experiments were conducted to extract cobalt and nickel from aqueous solutions of 0.5 and 0.5 mg/mL, respectively, by mixing equal amounts of organic and aqueous phases in a separatory funnel. The conditions for extraction (solution pH, extraction time, temperature, solution pH, saponification ratio, and solvent concentration) were then explored. To adjust the pH (0.5–4.5) of the aqueous solution, diluted HCl or NaOH was added before equilibration. The equilibrium pH of the aqueous phase, which had been divided after phase disengagement, was determined using the pH meter.

To ascertain the concentration of nickel and cobalt ions in aqueous phases before and after extraction, inductively coupled plasma-optical emission spectroscopy (ICP-OES, Agilent Technologies, Santa Clara, CA, USA) with an SPS3 autosampler and ICP Expert software 2.0.5 was employed. Working conditions of ICP-OES are listed in Table 1. Analytical-grade reagents were then used to prepare stock solutions of cobalt chloride (0.5 mg/mL Co.), nickel chloride (0.5 mg/mL Ni.), and a mixture of cobalt chloride and nickel chloride in which concentrations of them were both 0.5 mg/mL. To guarantee constant ionic strength, all extraction experiments were conducted in a 1 M NaCl solution.

Table 1. Optima instrumental parameters for ICP-OES.

Parameter	Optima Condition
Plasma gas flow rate (Ar)/(L/min)	15
Auxiliary gas flow (Ar)/(L/min)	0.15
Atomizer gas flow (Ar)/(L/min)	0.50
Pump injection volume/(mL/min)	1.5
Ni and Co analysis line/(nm)	216.5, 213.6

To calculate the concentration of Co and Ni ions in the organic phase, the difference between the aqueous phase's metal ion concentrations before and after extraction was measured.

The concentrations of P507 and QP–IL, ranging from 2 to 40% were used for the separation of Co and Ni. The solution pH, extraction time, saponification ratio, and temperature were also analyzed. The percentage of extraction E, distribution ratio D, and separation factor β were obtained by Equations (1)–(3), respectively.

$$E = \frac{C_a - C_e}{C_a} \tag{1}$$

$$D = \frac{C_o}{C_e} \tag{2}$$

$$\beta_{Co/Ni} = \frac{D_{Co}}{D_{Ni}} \tag{3}$$

where C_a stands for the original metal ion concentration in the aqueous phase before extraction and C_e is the equilibrium metal concentration in the aqueous phase after extraction. C_o stands for the equilibrium metal concentration in the organic phase. D_{Co} and D_{Ni} represent the distribution rates of *Co* and *Ni*, respectively.

2.4. Characterization

The structures of synthesized compounds were identified by Nuclear Magnetic Resonance Spectroscopy (NMR) and Fourier-Transform Spectroscopy (FT-IR). NMR spectra of QP–IL were acquired on an AVANCE III HD600 (Bruker, Fällanden, Switzerland) in d6-DMSO solution. FTIR analysis was performed on a Nicolet 380 spectrometer (Thermo Fisher Scientific, Waltham, MA, USA) by mixing the samples with potassium bromide (KBr) (0.5% w/w to KBr) in a range of 4000–400 cm^{-1} with an optical resolution of 4 cm^{-1} and an accumulation of 32 scans.

3. Results

3.1. FTIR Spectra of QP–IL

To elucidate the structure of QP–IL, we compared the FT-IR spectra of lignin, QAL and QP–IL (Figure 1 and Table 2).
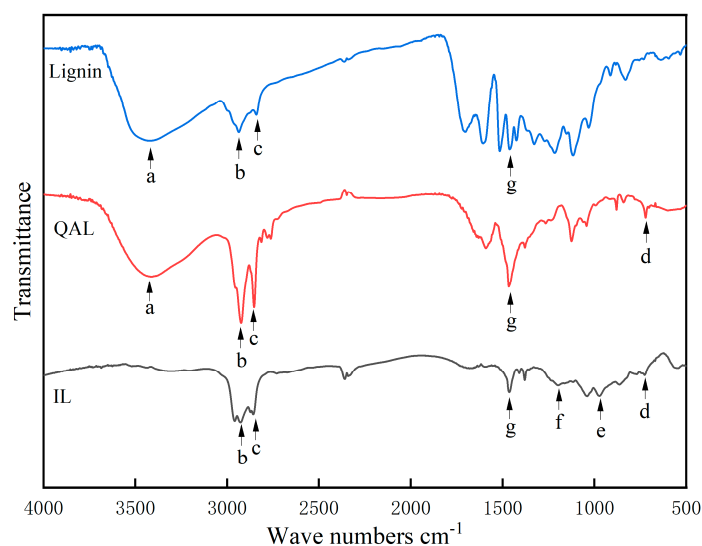
Figure 1. FTIR analysis of lignin, quaternary ammonium lignin, and ionic liquid.

The peak at 3430 cm^{-1}, attributed to the stretching vibration of the hydroxyl group, was absent in QP–IL, unlike lignin and QAL spectra. The absorption peaks at 2926 and 2856 cm^{-1} correspond to the C-H stretching vibrations of long-chain alkyl groups, which are significantly stronger compared to those observed in lignin [69]. The intensity of the C-N bond stretching vibration absorption peak at 721 cm^{-1} was notably reduced in QP–IL due to

quaternary ammonium compound formation. A small absorption peak ranging from 1000 to 910 cm^{-1} is consistent with the presence of quaternary ammonium salt. This suggests a preliminary reaction between lignin and dimethyltetradecylamine. Additionally, a P=O band stretching vibration absorption peak is observed at 1196 cm^{-1} [70], while phosphorus hydroxyl group vibrations are seen at 972 cm^{-1} (f, e, respectively), indicating distinctive groups within the molecular structure of QP–IL. Notably, a phenolic ring vibration is observed at 1462 cm^{-1} (g) in lignin, QAL, and QP–IL. All the changes in C-N, -OH, P-OH, and P=O bands may be attributed to interactions occurring between quaternary ammonium lignin and P507 at the molecular level.

**Table 2.** FTIR assignments correspondence.

	Wave Numbers	Characteristic Groups
a	3430 cm^{-1}	-OH (benzene ring)
b	2926 cm^{-1}	C-H of long-chain alkyl group
c	2856 cm^{-1}	
d	721 cm^{-1}	C-N bond
e	972 cm^{-1}	P-OH
f	1196 cm^{-1}	P=O
g	1462 cm^{-1}	phenolic ring
	1000~910 cm^{-1}	quaternary ammonium salt

3.2. NMR Spectroscopic Characterization of QP–IL

NMR was used to confirm the chemical structure of the QP–IL product.

^{1}H NMR (600 MHz, DMSO-d6) δ 6.70-6.80 (t, 3H), 4.06 (s, 4H), 3.77 (s, 3H), 3.42 (s, 4H), 3.15 (s, 6H), 2.11 (s, 3H), 1.82 (s, 6H), 1.26 (s, 40H), 0.88 (s, 15H).

The ^{1}H-NMR spectra of QP–IL are presented in Figure 2. The analysis of the ^{1}H NMR spectrum revealed that 2.50 ppm was assigned to the DMSO protons, while the aromatic protons exhibited signals between 6.70 and 6.80 ppm. Methoxyl protons were associated with a signal at 3.77 ppm, and the adjacent carbon atoms to N and O atoms showed signals at 3.42 and 4.06, respectively. The proton close to the nitrogen atom in the methyl group was identified by a signal at 3.15 ppm, whereas the proton on the terminal alkyl chain methyl group appeared at 0.88 ppm. The methylene protons on the long fatty chain were detected at a chemical shift of 1.37 ppm. In addition, it was evident from the obtained results that lignin and N, N-dimethyltetradecylamine formed an epichlorohydrin-bonded product with p507, existing as anionic liquid rather than free ions.
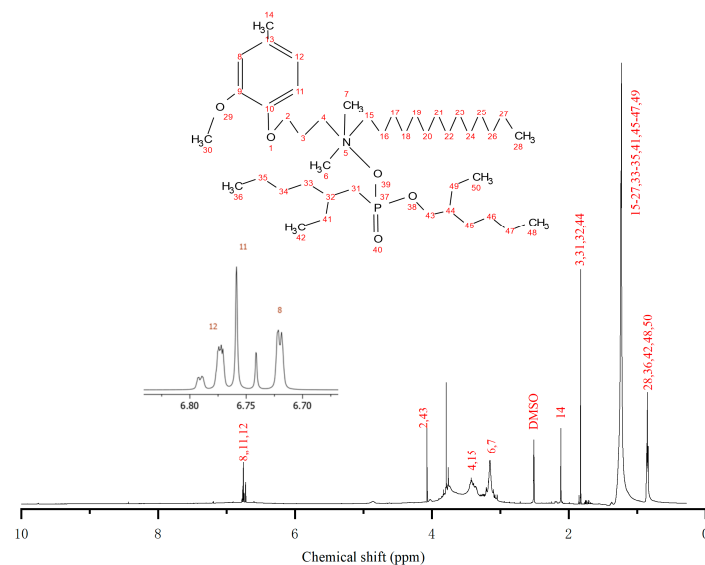

Figure 2. ^{1}H NMR spectrum of QP–IL in DMSO–d6.

3.3. Effect of Different Factors on Extraction for Co and Ni

3.3.1. Influence of Time on the Extraction

The influence of time on the extraction rate is demonstrated in Figure 3. By examining the extraction rates and $\beta_{Co/Ni}$ at intervals ranging from 1 to 15 min, a solution with a Co/Ni ratio of 1:1 and an initial pH of 3.5 was employed. It is evident that time significantly affects the effectiveness of Co and Ni extraction, as depicted in Figure 3. As time progresses, both the extraction ratio of Ni with P507 and QP–IL steadily increase. In contrast, the percent extraction of Co rapidly rises from 6.12% to 99.08%, similar to that observed for p507. Notably, a higher extraction ratio of Co with P507 and QP–IL compared to Ni is observed, particularly after an extraction time exceeding 4 min. At a time point of 10 min, the equilibrium concentration for Co reached levels of 98.55% and 99.34% using P507 and QP–IL, respectively; these values were more effective than those achieved for Ni individually. Furthermore, it should be noted that the $\beta_{Co/Ni}$ value for p507 is considerably lower than that obtained for QP–IL, reaching its highest value at a time point of ten minutes (1142).
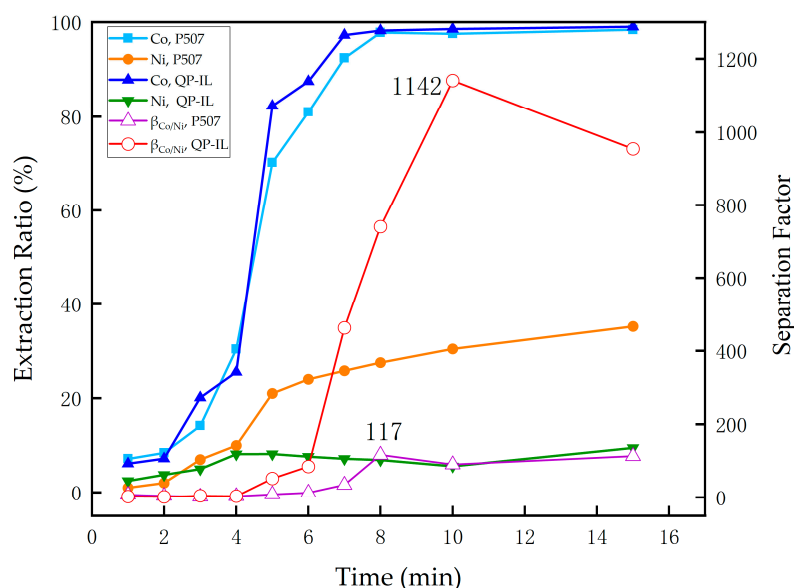
Figure 3. The extraction percentage of Co and Ni in chloride solution at various time points (organic phase: 30% (*v/v*) P507 or QP–IL in kerosene; aqueous phase: C_{Co} = 0.5 mg/mL, C_{Ni} = 0.5 mg/mL, pH$_{initial}$ = 3.5; room temperature; O = organic phase; A = aqueous phase, A/O = 1:1).

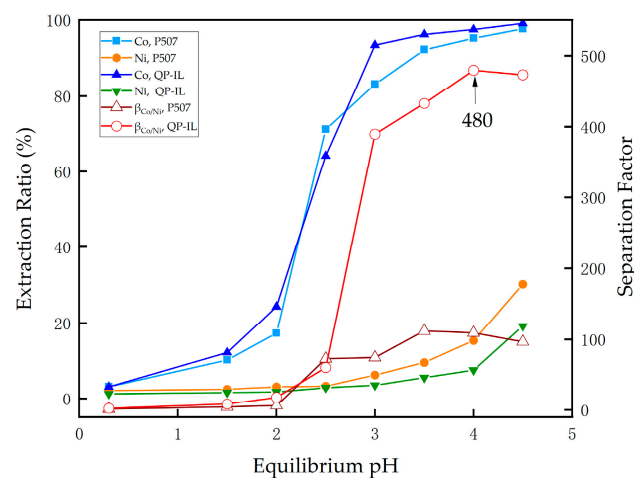3.3.2. Effect of Temperature on Extraction

The investigation of temperature's influence on Co/Ni separation is imperative due to significant temperature disparities across different regions. Extraction rates and $\beta_{Co/Ni}$ values were measured at various temperatures ranging from 25 °C to 85 °C in a solution with a Co/Ni ratio of 1:1, extractant concentration of 30%, and pH of 3.5. Figure 4 illustrates the obtained results. With increasing temperature, the extraction efficiency for Co gradually increased, while Ni extraction ratios remained relatively low and stable. At 85 °C, the highest Co extraction ratio achieved with P507 was recorded as 86.11%. Similarly, the separation efficiency of Co using QP–IL also improved with rising temperature, reaching its peak $\beta_{Co/Ni}$ value at 85 °C; however, it required multiple stages for effective separation between Co and Ni as the extraction ratio only reached up to 92.57%. Notably, there was minimal variation in $\beta_{Co/Ni}$ within the temperature range of 55 °C to 85 °C; thus, maintaining an extraction temperature of around 55 °C can effectively reduce energy consumption without compromising separation efficiency. These findings indicate that both extractants exhibit excellent thermal stability and higher temperatures are advantageous for efficient extraction of both Co and Ni.
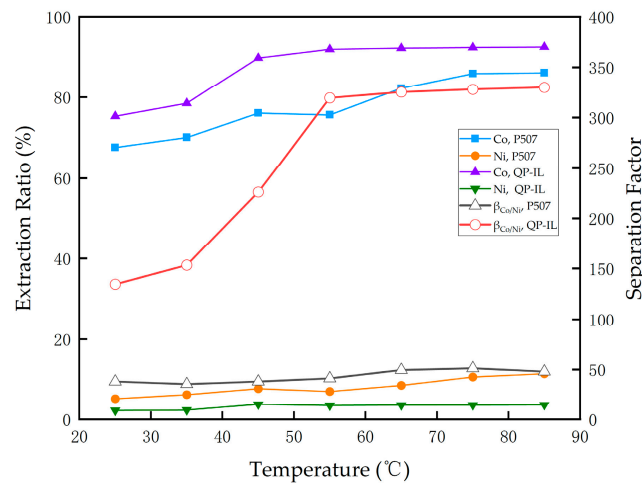
Figure 4. Effect of temperature on extraction efficiency and separation factor. (Organic phase: 30% (*v/v*) P507 or QP–IL in kerosene; aqueous phase: C_{Co} = 0.5 mg/mL, C_{Ni} = 0.5 mg/mL, pH$_{initial}$ = 3.5, room temperature; A/O = 1:1).

### 3.3.3. Effect of Equilibrium pH on Extraction Behavior

Experiments were conducted to investigate the percent extraction and selectivity of P507 and QP–IL for the primary metals Co and Ni. The correlations between equilibrium pH and extraction ratios of Co and Ni are illustrated in Figure 5. It is evident that the extraction of Ni was relatively low, with minimal influence from pH variations. Furthermore, it can be observed from the figure that both P507 and QP–IL exhibited a preference for extracting Co in acidic solutions, particularly when the pH value exceeded 3.0. At pH values of 3.0, 3.5, 4.0, and 4.5, the extraction ratios of Co using QP–IL reached 93.43%, 96.22%, 97.51%, and 99.12%, respectively, while those using P507 were measured at 83.21%, 92.22%, 95.21% and,97.67%. Compared to QP–IL, P507 demonstrated a similar trend in terms of Co and Ni extraction but with lower overall efficiency levels. To obtain comparable data under identical extraction conditions, $\beta_{Co/Ni}$ values were determined for both P507 and QP–IL. Notably, the separation factor ($\beta_{Co/Ni}$) for cobalt over nickel was consistently higher for QP–IL compared to P507. The highest $\beta_{Co/Ni}$ value was observed at pH4.0 using QP–IL, whereas it occurred at pH3.5 when employing P507(Hollow regular triangle). These results indicate that QP–IL exhibits superior selectivity towards Co over Ni.

Figure 5. Effect of equilibrium pH on extraction efficiency and separation factor. (Organic phase: 30% (*v/v*) P507 or QP–IL in kerosene; aqueous phase: C_{Co} = 0.5 mg/mL, C_{Ni} = 0.5 mg/mL, room temperature; A/O = 1:1).

3.3.4. Effect of Saponification on Extraction of Co and Ni

The impact of the saponification ratio on the extraction efficiency of cobalt and nickel from P507 is demonstrated in Figure 6. Initially, the saponification ratio increased dramatically from 1.42% to 99.55%, after which it stabilized. The $\beta_{Co/Ni}$ value of P507 exhibited an initial increase followed by a decrease, with a maximum value of 2696 achieved at a saponification ratio of 40%. As depicted in Figure 5, the lower the equilibrium pH, the lesser amounts of Co and Ni were separated. It has been established that organo-phosphorus acid extractant (P507) releases H^+ during Co and Ni extraction [33], leading to pH reduction. Therefore, saponification was necessary to maintain a relatively low equilibrium pH value. The saponification of both P507 and QP–IL was carried out in this section by adding NaOH at different saponification ratios.
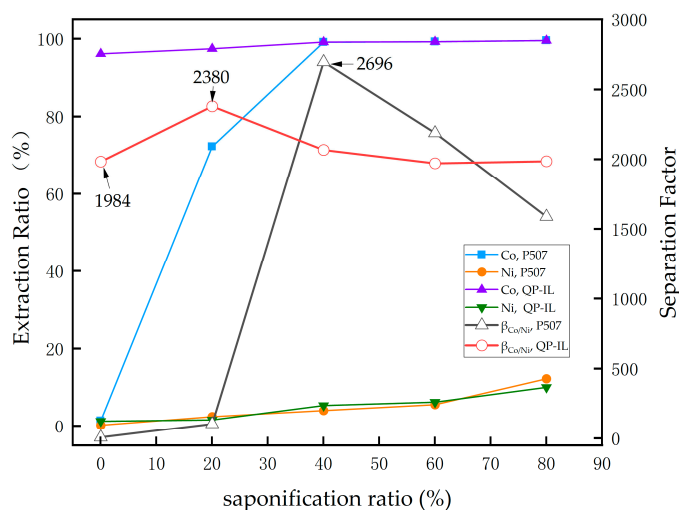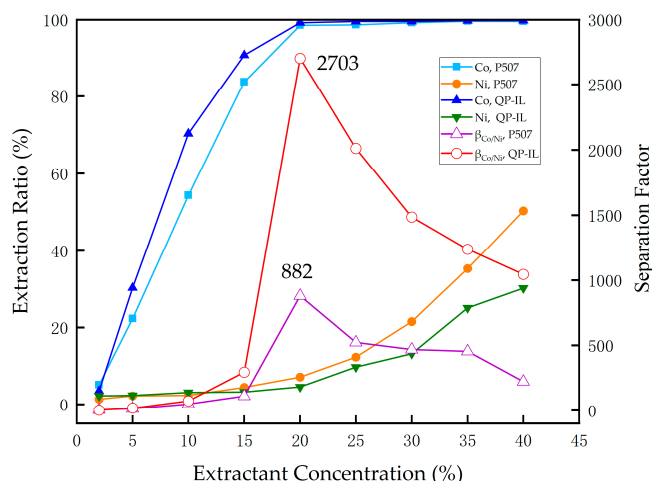

Figure 6. Effect of saponification ratio on Co/Ni separation. (Organic phase: 30% (*v*/*v*) P507 or QP–IL in kerosene; aqueous phase: C_{Co} = 0.5 mg/mL, C_{Ni} = 0.5 mg/mL, pH$_{initial}$ = 3.5, room temperature; A/O = 1:1).

As to QP–IL, its extraction ratio and separation factor for cobalt and nickel showed minimal variation with changing saponification ratios. The highest $\beta_{Co/Ni}$ value obtained was 2380 at a saponification ratio of 20%. These results indicate that under certain conditions, P507 exhibits superior separation performance compared to QP–IL; however, it should be noted that unsaponified QP–IL still achieved a $\beta_{Co/Ni}$ value as high as 1984. Considering factors such as the saponification process itself, the consumption of acid and base reagents, as well as treatment requirements for generated wastewater during the process, QP–IL emerges as a more favorable choice for practical production.

3.3.5. Effect of Concentration on Extraction of Co and Ni

The extraction capacity of P507 for cobalt is significantly higher than that for nickel [71]. As shown in the Figure 7, with the increase in concentration of P507 and QP–IL from 2% to 40%, the extraction ratios of cobalt increased rapidly, while the extraction ratio of nickel changed gradually. At a concentration of 20%, the extraction ratios of cobalt were 98.54% and 99.23% for P507 and QP–IL, respectively. When the concentration reached 40%, almost exclusive extraction of cobalt occurred, but there was a sudden surge in nickel extraction percentages beyond 20%. Therefore, it can be observed from the figure that there was a significant variation in $\beta_{Co/Ni}$ between the two extractants, particularly at a concentration of 20%. The results clearly demonstrate that at a QP–IL concentration of 20%, an optimal separation coefficient (β) value of Ni and Co was achieved at 2703. This finding indicates that under identical experimental conditions, QP–IL exhibits superior separation selectivity compared to P507.

Figure 7. Effect of extractant concentration on extraction behavior. (Organic phase:30% (*v/v*) P507 or QP–IL in kerosene; aqueous phase: C_{Co} = 0.5 mg/mL, C_{Ni} = 0.5 mg/mL, pH$_{initial}$ = 4.5, room temperature; A/O = 1:1).

4. Conclusions

In this study, a different process for the high value-added utilization of lignin was established: a new ionic liquid with quaternary ammonium lignin which can act as QP–IL for the extraction of Co and Ni were synthesized. Structural identification was conducted using spectroscopy techniques including 1HNMR and FT-IR. Two different extractants, P507 and QP–IL, were selected to investigate the effect of extraction time, temperature, saponification, pH value, and extractant concentration on the extraction behavior of Co and Ni in the mixed solution. The key findings are summarized as follows:

The extraction ratios for cobalt and nickel both exhibited an increasing trend over time, with Co demonstrating significantly higher values compared to Ni. At a duration of 10 min, the maximum extraction ratios achieved were 98.55% and 99.34% for Co using P507 and QP–IL, respectively, while the corresponding $\beta_{Co/Ni}$ value reached its peak at 1142 in QP–IL.

The extraction capacity of QP–IL for Co exceeded that of P507, demonstrating its superior performance. The elevation of temperature proved to be beneficial for the extraction process, enhancing both efficiency and effectiveness. Notably, at a temperature of 85 °C in QP–IL, the maximum extraction ratio reached an impressive 92.57%, with a $\beta_{Co/Ni}$ value of 330.

The pH value exerts a significant influence on the extraction ratio and separation efficiency. Both Co and Ni exhibited increased extraction ratios as the pH value increased. At a pH of 4.5, the extraction ratios for Co reached 97.67% and 99.12% in P507 and QP–IL, respectively. However, the optimal $\beta_{Co/Ni}$ value of 480 was observed at pH 4.0 in QP–IL due to the reduced extraction ratio for Ni.

The saponification ratio has a significant impact on the extraction percentage of cobalt and nickel from P507. The highest $\beta_{Co/Ni}$ value achieved was 2696 at a saponification ratio of 40%. Unsaponified QP–IL also demonstrates excellent separation capability.

The extraction ratio and separation factor are significantly influenced by the concentration of the extractant; as the concentration increases, so does the extraction of cobalt ions into the organic phase. If the concentration persists, the majority of cobalt ions will be drawn into the organic phase. The optimal separation results were observed in a 40% QP–IL solution.

According to the aforementioned experimental results, the selectivity of QP–IL for Co renders it a promising extractant for efficient separation from weak acid solutions. However, achieving optimal separation efficiency is contingent upon various factors and necessitates further research.

According to the abovementioned experimental results, the selectivity of the QP–IL for Co can be used as a good extractant for separating them from the weak acid solution. However, the separation efficiency is related to many factors, and further research is needed.

Author Contributions: Conceptualization, methodology, formal analysis, writing—original draft preparation, G.L.; investigation, writing—review and editing, W.X. All authors have read and agreed to the published version of the manuscript.

Data Availability Statement: Upon reasonable request, the corresponding author can provide the data of this study.

Conflicts of Interest: No conflicts of interest are declared by the authors.

References

1. Nasrollahzadeh, M.; Ghasemzadeh, M.; Gharoubi, H.; Nezafat, Z. Progresses in polysaccharide and lignin-based ionic liquids: Catalytic applications and environmental remediation. *J. Mol. Liq.* **2021**, *342*, 117559. [CrossRef]
2. Das, A.K.; Mitra, K.; Conte, A.J.; Sarker, A.; Chowdhury, A.; Ragauskas, A.J. Lignin-A green material for antibacterial application— A review. *Int. J. Biol. Macromol.* **2024**, *261*, 129753. [CrossRef]
3. Yang, G.; Gong, Z.; Zhou, B.; Luo, X.; Liu, J.; Du, G.; Zhao, C.; Shuai, L. Hydrodeoxygenation of condensed lignins followed by acid-mediated methylolation enables preparation of lignin-based wood adhesives. *Green Chem.* **2024**, *26*, 753–759. [CrossRef]
4. Beaucamp, A.; Muddasar, M.; Culebras, M.; Collins, M.N. Sustainable lignin-based carbon fibre reinforced polyamide composites: Production, characterisation and life cycle analysis. *Compos. Commun.* **2024**, *45*, 101782. [CrossRef]
5. Zheng, Z.; Zhang, H.; Qian, K.; Li, L.; Shi, D.; Zhang, R.; Li, L.; Yu, H.; Zheng, C.; Xie, S.; et al. Wood structure-inspired injectable lignin-based nanogels as blood-vessel-embolic sustained drug-releasing stent for interventional therapies on liver cancer. *Biomaterials* **2023**, *302*, 122324. [CrossRef] [PubMed]
6. Kim, Y.; Shim, J.; Choi, J.-W.; Jin Suh, D.; Park, Y.-K.; Lee, U.; Choi, J.; Ha, J.-M. Continuous-flow production of petroleum-replacing fuels from highly viscous Kraft lignin pyrolysis oil using its hydrocracked oil as a solvent. *Energy Convers. Manag.* **2020**, *213*, 112728. [CrossRef]
7. Sun, S.; Bai, R.; Gu, Y. From waste biomass to solid support: Lignosulfonate as a cost-effective and renewable supporting material for catalysis. *Chemistry* **2014**, *20*, 549–558. [CrossRef] [PubMed]
8. Nasrollahzadeh, M.; Shafiei, N.; Nezafat, Z.; Bidgoli, N.S.S. Recent progresses in the application of lignin derived (nano)catalysts in oxidation reactions. *Mol. Catal.* **2020**, *489*, 110942. [CrossRef]
9. Sugiarto, S.; Leow, Y.; Tan, C.L.; Wang, G.; Kai, D. How far is Lignin from being a biomedical material? *Bioact. Mater.* **2022**, *8*, 71–94. [CrossRef]
10. Burzynska, L.; Gumowska, W. Hydrometallurgical recovery of copper and cobalt from reduction-roasted copper converter slag. *Miner. Eng.* **2009**, *22*, 88–95. [CrossRef]
11. Prakash, U.; Bhagat, L.; Abhilash; Zhao, H.; van Hullebusch, E.D. Processing of Waste Copper Converter Slag Using Organic Acids for Extraction of Copper, Nickel, and Cobalt. *Minerals* **2020**, *10*, 290. [CrossRef]
12. Ziyadanogullari, B. Recovery of Copper and Cobalt from Concentrate and Converter Slag. *Sep. Sci. Technol.* **2000**, *35*, 1963–1971. [CrossRef]
13. Arslan, F. Recovery of copper, cobalt, and zinc from copper smelter and converter slags. *Hydrometallurgy* **2002**, *67*, 1–7. [CrossRef]
14. Gumowska, W.; Rudnik, E.; Partyka, J. Mechanism of the anodic dissolution of Cu70-Co4-Fe14-Pb7 alloy originated from reduced copper converter slag in an ammoniacal solution: Recovery of copper and cobalt. *Hydrometallurgy* **2008**, *92*, 34–41. [CrossRef]
15. Das, C.; Pandey, B.D. Leaching of copper, nickel and cobalt from Indian Ocean manganese nodules by Aspergillus niger. *Hydrometallurgy* **2010**, *105*, 89–95. [CrossRef]
16. Verma, J.K. Extraction of copper, nickel and cobalt from the leach liquor of manganese-bearing sea nodules using LIX 984N and ACORGA M5640. *Miner. Eng.* **2011**, *24*, 959–962. [CrossRef]
17. Dreano, A.; Fouvry, S.; Guillonneau, G. Understanding and formalization of the fretting-wear behavior of a cobalt-based alloy at high temperature. *Wear* **2020**, *452*, 203297. [CrossRef]
18. Amsarajan, S.; Jagirdar, B.R. Air-stable magnetic cobalt-iron (Co_7Fe_3) bimetallic alloy nanostructures via co-digestive ripening of cobalt and iron colloids. *J. Alloys Compd.* **2020**, *816*, 152632. [CrossRef]
19. Agarwal, A.; Jo, Y.T.; Rana, M.; Shin, D.; Park, J.-H. Chlorinated polyvinyl chloride (CPVC) assisted leaching of lithium and cobalt from spent lithium-ion battery in subcritical water. *J. Hazard. Mater.* **2020**, *393*, 122367. [CrossRef]
20. Fu, Y.; He, Y.; Qu, L.; Feng, Y.; Li, J.; Liu, J.; Zhang, G.; Xie, W. Enhancement in leaching process of lithium and cobalt from spent lithium-ion batteries using benzenesulfonic acid system. *Waste Manag.* **2019**, *88*, 191–199. [CrossRef]
21. Hu, J.; Zhang, W.; Chen, Y.; Wang, C. Efficient and economical recovery of lithium, cobalt, nickel, manganese from cathode scrap of spent lithium-ion batteries. *J. Clean. Prod.* **2018**, *204*, 437–446. [CrossRef]

22. Kumari, A.; Jha, A.K.; Kumar, V.; Hait, J.; Pandey, B.D. Recovery of lithium and cobalt from waste lithium ion batteries of mobile phone. *Waste Manag.* **2013**, *33*, 1890–1897. [CrossRef]

23. Bhanvase, B.A.; Sonawane, S.H. Investigation on liquid emulsion membrane (LEM) prepared with hydrodynamic cavitation process for cobalt (II) extraction from wastewater. *Sep. Purif. Technol.* **2020**, *237*, 116385. [CrossRef]

24. Wang, W.-Y.; Yen, C.H.; Lin, J.-L.; Xu, R.-B. Recovery of high-purity metallic cobalt from lithium nickel manganese cobalt oxide (NMC)-type Li-ion battery. *J. Mater. Cycles Waste Manag.* **2019**, *21*, 300–307. [CrossRef]

25. Biswal, B.K.; Jadhav, U.U.; Madhaiyan, M.; Ji, L.; Yang, E.-H.; Cao, B. Biological Leaching and Chemical Precipitation Methods for Recovery of Co and Li from Spent Lithium-Ion Batteries. *ACS Sustain. Chem. Eng.* **2018**, *6*, 12343–12352. [CrossRef]

26. Feng, X.N.; Sun, J.; Ouyang, M.G.; He, X.M.; Lu, L.U.; Han, X.B.; Fang, M.; Peng, H. Characterization of large format lithium ion battery exposed to extremely high temperature. *J. Power Sources* **2014**, *272*, 457–467. [CrossRef]

27. Fu, G.; Wang, Z.; Hall, P. Recovering lithium cobalt oxide, aluminium, and copper from spent lithium-ion battery via attrition scrubbing. *J. Clean. Prod.* **2020**, *260*, 120869. [CrossRef]

28. Golmohammadzadeh, R.; Faraji, F.; Rashchi, F. Recovery of lithium and cobalt from spent lithium ion batteries (LIBs) using organic acids as leaching reagents: A review. *Resour. Conserv. Recycl.* **2018**, *136*, 418–435. [CrossRef]

29. Ichlas, Z.T.; Mubarok, M.Z.; Magnalita, A.; Vaughan, J.; Sugiarto, A.T. Processing mixed nickel-cobalt hydroxide precipitate by sulfuric acid leaching followed by selective oxidative precipitation of cobalt and manganese. *Hydrometallurgy* **2020**, *191*, 105185. [CrossRef]

30. Wen, J.; Tran, T.T.; Lee, M.S. Comparison of separation of Mn(II), Co(II), and Ni(II) by oxidative precipitation between chloride and sulfate solutions. *Physicochem. Probl. Miner. Process.* **2024**, *60*, 183029. [CrossRef]

31. Dhiman, S.; Gupta, B. Partition studies on cobalt and recycling of valuable metals from waste Li-ion batteries via solvent extraction and chemical precipitation. *J. Clean. Prod.* **2019**, *225*, 820–832. [CrossRef]

32. Han, B.; Li, S.; Chang, D.; Li, J.; Li, T.; Yang, S.; Chen, Y.; Zhang, H. Efficient phenyl phosphate ester extractant synthesis and solvent extraction performance evaluation for transition metals. *Sep. Purif. Technol.* **2024**, *336*, 126251. [CrossRef]

33. Abo Atia, T.; Deferm, C.; Machiels, L.; Khoshkhoo, M.; Riaño, S.; Binnemans, K. Solvent Extraction Process for Refining Cobalt and Nickel from a "Bulk Hydroxide Precipitate" Obtained by Bioleaching of Sulfidic Mine Tailings. *Ind. Eng. Chem. Res.* **2023**, *62*, 17947–17958. [CrossRef]

34. Rodrigues, I.R.; Deferm, C.; Binnemans, K.; Riaño, S. Separation of cobalt and nickel via solvent extraction with Cyanex-272: Batch experiments and comparison of mixer-settlers and an agitated column as contactors for continuous counter-current extraction. *Sep. Purif. Technol.* **2022**, *296*, 121326. [CrossRef]

35. Li, K.; Li, Q.; Yang, Y.; Liu, X.; Jiang, T. Kinetic studies of gold leaching from a gold concentrate calcine by thiosulfate with cobalt-ammonia catalysis and gold recovery by resin adsorption from its pregnant solution. *Sep. Purif. Technol.* **2019**, *213*, 368–377. [CrossRef]

36. Zioui, D.; Arous, O.; Mameri, N.; Kerdjoudj, H.; Sebastian, M.S.; Vilas, J.L.; Nunes-Pereira, J.; Lanceros-Mendez, S. Membranes based on polymer miscibility for selective transport and separation of metallic ions. *J. Hazard. Mater.* **2017**, *336*, 188–194. [CrossRef] [PubMed]

37. Yang, Y.; Song, W.; Ferrier, J.; Liu, F.; Csetenyi, L.; Gadd, G.M. Biorecovery of cobalt and nickel using biomass-free culture supernatants from Aspergillus niger. *Appl. Microbiol. Biotechnol.* **2020**, *104*, 417–425. [CrossRef] [PubMed]

38. Swain, B.; Cho, S.-S.; Lee, G.H.; Lee, C.G.; Uhm, S. Extraction/Separation of Cobalt by Solvent Extraction: A Review. *Appl. Chem. Eng.* **2015**, *26*, 631–639. [CrossRef]

39. Kumari, A.; Panda, R.; Lee, J.Y.; Thriveni, T.; Jha, M.K.; Pathak, D.D. Extraction of rare earth metals (REMs) from chloride medium by organo-metallic complexation using D2EHPA. *Sep. Purif. Technol.* **2019**, *227*, 115680. [CrossRef]

40. Pavon, S.; Fortuny, A.; Coll, M.T.; Sastre, A.M. Solvent extraction modeling of Ce/Eu/Y from chloride media using D2EHPA. *Aiche J.* **2019**, *65*, e16627. [CrossRef]

41. Yin, S.; Zhang, L.; Peng, J.; Li, S.; Ju, S.; Zhang, L. Microfluidic solvent extraction of La (III) with 2-ethylhexyl phosphoric acid-2-ethylhexyl ester (P507) by a microreactor. *Chem. Eng. Process. Process Intensif.* **2015**, *91*, 1–6. [CrossRef]

42. Zhang, L.; Hessel, V.; Peng, J.; Wang, Q.; Zhang, L. Co and Ni extraction and separation in segmented micro-flow using a coiled flow inverter. *Chem. Eng. J.* **2017**, *307*, 1–8. [CrossRef]

43. Irannajad, M.; Haghighi, H.K.; Nasirpour, Z. New Solvent Extraction Process of Nickel and Copper by D2EHPA in the Presence of Carboxylates. *Trans. Indian Inst. Met.* **2020**, *73*, 1053–1063. [CrossRef]

44. Nadimi, H.; Haghshenas Fatmehsari, D.; Firoozi, S. Separation of Ni and Co by D2EHPA in the Presence of Citrate Ion. *Metall. Mater. Trans. B* **2017**, *48*, 2751–2758. [CrossRef]

45. Abu Elgoud, E.M.; Ismail, Z.H.; El-Nadi, Y.A.; Aly, H.F. Separation of cerium(IV) and yttrium(III) from citrate medium by solvent extraction using D2EHPA in kerosene. *Chem. Pap.* **2020**, *74*, 2461–2469. [CrossRef]

46. Abu Elgoud, E.M.; Ismail, Z.H.; El-Nadi, Y.A.; Abdelwahab, S.M.; Aly, H.F. Extraction of Some Rare Earth Elements (La, Pr and Er) from Citrate Medium Using D2EHPA in kerosene. *Arab. J. Nucl. Sci. Appl.* **2019**, *52*, 74–85. [CrossRef]

47. Jafari, H.; Abdollahi, H.; Gharabaghi, M.; Balesini, A.A. Solvent extraction of zinc from synthetic Zn-Cd-Mn chloride solution using D2EHPA: Optimization and thermodynamic studies. *Sep. Purif. Technol.* **2018**, *197*, 210–219. [CrossRef]

48. Habibpour, R.; Dargahi, M.; Kashi, E.; Bagherpour, M. Comparative study on Ce (III) and La (III) solvent extraction and separation from a nitric acid medium by D2EHPA and Cyanex272. *Metall. Res. Technol.* **2018**, *115*, 207. [CrossRef]

49. Mohapatra, P.K.; Raut, D.R.; Sengupta, A. Extraction of uranyl ion from nitric acid medium using solvent containing TOPO and its mixture with D2EHPA in room temperature ionic liquids. *Sep. Purif. Technol.* **2014**, *133*, 69–75. [CrossRef]
50. Torkaman, R.; Asadollahzadeh, M.; Torab-Mostaedi, M.; Maragheh, M.G. Reactive extraction of cobalt sulfate solution with D2EHPA/TBP extractants in the pilot plant Oldshue-Rushton column. *Chem. Eng. Res. Des.* **2017**, *120*, 58–68. [CrossRef]
51. Sousa, C.D.; Nascimento, M.; Ferreira, I.L.S. Modeling of nickel extraction by D2EHPA in sulfuric media. *Rem-Rev. Esc. Minas* **2011**, *64*, 447–452.
52. Lin, L.; Wei, J.-H.; Wu, G.-Y.; Toyohisa, F.; Atsushi, S. Extraction studies of cobalt (II) and nickel (II) from chloride solution using PC88A. *Trans. Nonferrous Met. Soc. China* **2006**, *16*, 687–692.
53. Zhang, Y.; Man, R.-l.; Wang, H.; Liang, Y.-h. Extraction of cobalt with P507 and preparation of cobalt oxalate powders by ethane diacid stripping. *J. Cent. South Univ. (Sci. Technol.)* **2011**, *42*, 317–322.
54. Flett, D.S. Solvent extraction in hydrometallurgy: The role of organophosphorus extractants. *J. Organomet. Chem.* **2005**, *690*, 2426–2438. [CrossRef]
55. Kang, J.; Senanayake, G.; Sohn, J.; Shin, S.M. Recovery of cobalt sulfate from spent lithium ion batteries by reductive leaching and solvent extraction with Cyanex 272. *Hydrometallurgy* **2010**, *100*, 168–171. [CrossRef]
56. Tanong, K.; Tran, L.-H.; Mercier, G.; Blais, J.-F. Recovery of Zn (II), Mn (II), Cd (II) and Ni (II) from the unsorted spent batteries using solvent extraction, electrodeposition and precipitation methods. *J. Clean. Prod.* **2017**, *148*, 233–244. [CrossRef]
57. Qiu, L.N.; Pan, Y.H.; Zhang, W.W.; Gong, A.J. Application of a functionalized ionic liquid extractant tributylmethylammonium dibutyldiglycolamate ([A336][BDGA]) in light rare earth extraction and separation. *PLoS ONE* **2018**, *13*, e0201405. [CrossRef] [PubMed]
58. Wang, Y.; Wang, Y.D.; Ding, Y.; Chen, J.; Liu, Y. Microcapsules containing ionic liquid [A336][P507] for La3+/Sm3+/Er3+ recovery from dilute aqueous solution. *J. Rare Earths* **2016**, *34*, 1260–1268. [CrossRef]
59. Fernandes, A.; Afonso, J.C.; Dutra, A.J.B. Separation of nickel(II), cobalt(II) and lanthanides from spent Ni-MH batteries by hydrochloric acid leaching, solvent extraction and precipitation. *Hydrometallurgy* **2013**, *133*, 37–43. [CrossRef]
60. Fernandes, A.; Afonso, J.C.; Bourdot Dutra, A.J. Hydrometallurgical route to recover nickel, cobalt and cadmium from spent Ni–Cd batteries. *J. Power Sources* **2012**, *220*, 286–291. [CrossRef]
61. Sarangi, K. Separation of copper, zinc, cobalt and nickel ions by supported liquid membrane technique using LIX 84I, TOPS-99 and Cyanex 272. *Sep. Purif. Technol.* **2008**, *59*, 169–174. [CrossRef]
62. Parija, C.; Reddy, B.; Sarma, P.B. Recovery of nickel from solutions containing ammonium sulphate using LIX 84-I. *Hydrometallurgy* **1998**, *49*, 255–261. [CrossRef]
63. Guimardes, A.S.; Silva, L.A.; Pereira, A.M.; Correia, J.C.G.; Mansur, M.B. Purification of concentrated nickel sulfuric liquors via synergistic solvent extraction of calcium and magnesium using mixtures of D2EHPA and Cyanex 272. *Sep. Purif. Technol.* **2020**, *239*, 116570. [CrossRef]
64. van Stee, J.; Hermans, G.; John, J.J.; Binnemans, K.; Van Gerven, T. Cobalt/nickel purification by solvent extraction with ionic liquids in millifluidic reactors: From single-channel to numbered-up configuration with solvent recycle. *Chem. Eng. J.* **2024**, *479*, 147234. [CrossRef]
65. Łukomska, A.; Wiśniewska, A.; Dąbrowski, Z.; Kolasa, D.; Luchcińska, S.; Domańska, U. Separation of cobalt, lithium and nickel from the "black mass" of waste Li-ion batteries by ionic liquids, DESs and organophosphorous-based acids extraction. *J. Mol. Liq.* **2021**, *343*, 117694. [CrossRef]
66. Boudesocque, S.; Viau, L.; Dupont, L. Selective Cobalt over Nickel separation using neat and confined ionic liquids. *J. Environ. Chem. Eng.* **2020**, *8*, 104319. [CrossRef]
67. Diabate, P.D.; Boudesocque, S.; Mohamadou, A.; Dupont, L. Separation of cobalt, nickel and copper with task-specific amido functionalized glycine-betaine-based ionic liquids. *Sep. Purif. Technol.* **2020**, *244*, 116782. [CrossRef]
68. Sun, X.; Ji, Y.; Liu, Y.; Chen, J.; Li, D. An engineering-purpose preparation strategy for ammonium-type ionic liquid with high purity. *AIChE J.* **2009**, *56*, 989–996. [CrossRef]
69. Xiong, P.; Zhang, Y.; Huang, J.; Bao, S.; Yang, X.; Shen, C. High-efficient and selective extraction of vanadium (V) with N235-P507 synergistic extraction system. *Chem. Eng. Res. Des.* **2017**, *120*, 284–290. [CrossRef]
70. Zhang, F.; Wu, W.; Bian, X.; Zeng, W. Synergistic extraction and separation of lanthanum (III) and cerium (III) using a mixture of 2-ethylhexylphosphonic mono-2-ethylhexyl ester and di-2-ethylhexyl phosphoric acid in the presence of two complexing agents containing lactic acid and citric acid. *Hydrometallurgy* **2014**, *149*, 238–243. [CrossRef]
71. Rao, M.J.; Zhang, T.; Li, G.H.; Zhou, Q.; Luo, J.; Zhang, X.; Zhu, Z.P.; Peng, Z.W.; Jiang, T. Solvent Extraction of Ni and Co from the Phosphoric Acid Leaching Solution of Laterite Ore by P204 and P507. *Metals* **2020**, *10*, 545. [CrossRef]